

Synthesis and Structural Characterization of Di-μ-Phenoxo-Bridged Dinuclear Iron(Ⅲ) Complexes with Ferromagnetic or Weak Antiferromagnetic Coupling

Masahiro Mikuriya,* Yoshihisa Kakuta, Ryoji Nukada, Takanori Kotera, and Tadashi Tokii†

Department of Chemistry, School of Science, Kwansei Gakuin University, Uegahara, Nishinomiya 662-8501

†Department of Chemistry and Applied Chemistry, Faculty of Science and Engineering, Saga University, Honjo 1, Saga 840-8502

(Received January 29, 2001)

Dinuclear phenoxo-bridged iron(Ⅲ) complexes with *N*-salicylidene-2-hydroxy-5-bromobenzylamine (H_2L^a), *N*-salicylidene-2-hydroxy-5-chlorobenzylamine (H_2L^b), and *N*-salicylidene-2-hydroxybenzylamine (H_2L^c): $[Fe_2(L^a)_2(CH_3CO_2)_2]$ (**1**), $[Fe_2(L^a)_2(C_6H_5CO_2)_2]$ (**2**), $[Fe_2(L^a)\{(CH_3)_3CCO_2\}_2]$ (**3**), $[Fe_2(L^a)_2\{(C_6H_5O)_2PO_2\}_2]$ (**4**), $[Fe_2(L^a)_2(CH_3COCHCOCH_3)_2]$ (**5**), $[Fe_2(L^b)_2(CH_3CO_2)_2]$ (**6**), and $[Fe_2(L^c)_2(CH_3CO_2)_2]$ (**7**), have been synthesized and characterized by measurements of the infrared and electronic spectra as well as the magnetic susceptibilities. Single-crystal X-ray analysis has revealed that all of the complexes are dinuclear iron(Ⅲ) complexes having a dinuclear iron(Ⅲ) core bridged by two phenoxo-oxygen atoms of the Schiff-base ligands. The magnetic-susceptibility data show that a ferromagnetic interaction is operative within a dinuclear core in **1**–**4**, **6**, and **7** with *J* values ranging from 0.17(5) to 1.56(15) cm^{-1}, whereas an antiferromagnetic coupling is operative in **5** with a *J* value of $-9.24(6)$ cm^{-1}. The magnetic properties are discussed in relation to the crystal structures.

Dinuclear iron complexes have been of wide interest and relevance to studies of biological iron-containing proteins.[1] Today, it is well known that dinuclear iron centers have important functional roles in the active sites of iron-containing proteins, such as hemerythrin, ribonucleotide reductase, methane monooxygenase, and purple acid phosphatases.[2] During the last decade, a large number of dinuclear iron complexes have been synthesized as models for biological systems. These complexes are interesting not only from a bioinorganic-chemical point of view, but also from a magneto-chemical stand point. As for dinuclear copper(Ⅱ) and chromium(Ⅲ) complexes, semiquantative relationships have been established between the magnetic exchange coupling constants and the structural parameters.[3] Several attempts to correlate the magnetic exchange parameters to the structural parameters have been made for dinuclear iron(Ⅲ) complexes.[4] Gorun and Lippard correlated the strength of antiferromagnetic coupling in dinuclear iron(Ⅲ) centers incorporating a ligand oxygen atom bridge with parameter *P*, defined as half the distance of the shortest superexchange pathway between the iron centers, according to the relation $-J = A\exp(BP)$, with $A = 8.763 \times 10^{11}$ and $B = -12.663$.[4a] However, there seems to exist no clear relationship between magnetic and structural parameters, such as *J* and M–O–M angles for iron systems. This may come from the fact that most of the reported dinuclear iron(Ⅲ) complexes are μ-oxo-bridged iron(Ⅲ) dimers containing μ-oxo-,[5] di-μ-oxo-,[6] μ-oxo-μ-carboxylato-,[7] μ-oxo-di-μ-carboxylato-,[8] μ-oxo-μ-carbonato-,[9] μ-oxo-di-μ-carbonato-,[10] μ-oxo-μ-molybdato-,[11] μ-oxo-μ-phosphato-,[12] and μ-oxo-μ-phosphinato-[13] bridges, and that examples of other types of dinuclear species are very limited.[14–18] As part of a continuing project on metal complexes with tridentate Schiff-base ligands,[19,20] we have reported on the synthesis and characterization of several manganese and vanadium complexes with *N*-salicylidene-2-hydroxybenzylamine and its substituted analogues. During this activity, we found that novel di-μ-phenoxo-bridged iron(Ⅲ) complexes are formed in reactions of these Schiff-base ligands with iron salts. It is important to develop syntheses of di-μ-phenoxo-bridged iron(Ⅲ) species with a view to studying the magneto-structural relationship for iron systems. Herein we report on the synthesis, magnetic properties, and crystal structures of dinuclear iron(Ⅲ) complexes with *N*-salicylidene-2-hydroxy-5-bromobenzylamine (H_2L^a), *N*-salicylidene-2-hydroxy-5-chlorobenzylamine (H_2L^b) and *N*-salicylidene-2-hydroxybenzylamine (H_2L^c). A preliminary account of this study was previously reported.[21]

Experimental

Synthesis of the Complexes. *o*-Hydroxybenzylamine was prepared by a published procedure.[22] 2-Hydroxy-5-chlorobenzylamine and 2-hydroxy-5-bromobenzylamine were synthesized according to a method reported by Yamaguchi.[23]

$[Fe_2(L^a)_2(CH_3CO_2)_2]$ (1). 2-Hydroxy-5-bromobenzylamine (20 mg, 0.099 mmol) and salicylaldehyde (12 mg, 0.098 mmol) were dissolved in 10 cm^3 of acetonitrile. The solution was stirred and heated at ca. 70 °C. To the resulting solution were successively added acetic acid (12 mg, 0.20 mmol), triethylamine (22 mg, 0.22 mmol), and iron(Ⅲ) chloride hexahydrate (27 mg, 0.10 mmol). After the reaction mixture had been stirred and filtered while hot, the filtrate was placed at room temperature for several

days. Black crystals were deposited and collected by filtration and dried in vacuo over P_2O_5: Yield, 26 mg (31%). Found: C, 45.94; H, 3.16; N, 3.53%. Calcd for $C_{32}H_{26}Br_2Fe_2N_2O_8$: C, 45.86; H, 3.13; N, 3.34%. IR (KBr, cm^{-1}) ν(C=N) 1615, $\nu_{as}(COO^-)$ 1538, $\nu_s(COO^-)$ 1400. μ_{eff} (295 K) per molecule/B.M. 8.64. Diffuse reflectance spectrum: λ_{max}/nm 255, 319, 509. Electronic spectrum in dmf (*N*,*N*-dimethylformamide): λ_{max}/nm (ε per Fe/dm^3 mol^{-1} cm^{-1}) 293 (10960), 418 (3130), 455sh (2880).

$[Fe_2(L^a)_2(C_6H_5CO_2)_2]$ (2). 2-Hydroxy-5-bromobenzylamine (20 mg, 0.099 mmol) and salicylaldehyde (12 mg, 0.098 mmol) were dissolved in acetonitrile (20 cm^3). While the solution was being stirred, sodium benzoate (29 mg, 0.20 mmol) and iron(III) chloride hexahydrate (27 mg, 0.10 mmol) were added, and the resulting solution was filtered. After the filtrate was allowed to stand for several days at room temperature, black crystals resulted, which were filtered and dried in vacuo over P_2O_5: Yield, 31 mg (32%). Found: C, 52.42; H, 2.91; N, 3.14%. Calcd for $C_{42}H_{30}Br_2Fe_2N_2O_8$: C, 52.43; H, 3.14; N, 2.91%. IR (KBr, cm^{-1}) ν(C=N) 1617, $\nu_{as}(COO^-)$ 1540, $\nu_s(COO^-)$ 1391. μ_{eff} (295 K) per molecule/B.M. 8.34. Diffuse reflectance spectrum: λ_{max}/nm 255, 318, 516. Electronic spectrum in dmf: λ_{max}/nm(ε per Fe/dm^3 mol^{-1} cm^{-1}) 290sh (4180), 420sh (1100), 470sh (790).

$[Fe_2(L^a)\{(CH_3)_3CCO_2\}_2]$ (3). After 2-hydroxy-5-bromobenzylamine (20 mg, 0.099 mmol) and salicylaldehyde (12 mg, 0.098 mmol) were dissolved in acetonitrile (10 cm^3), pivalic acid (20 mg, 0.20 mmol), triethylamine (30 mg, 0.30 mmol), and iron(III) chloride hexahydrate (27 mg, 0.10 mmol) were added. After the resulting solution was filtered, the filtrate was left standing for several days at room temperature to give black crystals. These were collected by filtration and dried in vacuo over P_2O_5: Yield, 34 mg (37%). Found: C, 49.34; H, 4.12; N, 3.09%. Calcd for $C_{38}H_{38}Br_2Fe_2N_2O_8$: C, 49.49; H, 4.15; N, 3.04%. IR(KBr, cm^{-1}) ν(C=N) 1618, $\nu_{as}(COO^-)$ 1518, $\nu_s(COO^-)$ 1413. μ_{eff} (295 K) per molecule/B.M. 8.37. Diffuse reflectance spectrum: λ_{max}/nm 254, 324, 510. Electronic spectrum in dmf: λ_{max}/nm(ε per Fe/dm^3 mol^{-1} cm^{-1}) 293 (11560), 420 (3200), 460sh (3120).

$[Fe_2(L^a)_2((C_6H_5O)_2PO_2)_2]$ (4). 2-Hydroxy-5-bromobenzylamine (20 mg, 0.099 mmol) and salicylaldehyde (12 mg, 0.098 mmol) were dissolved in a mixture of acetonitrile (15 cm^3) and *N*,*N*-dimethylformamide (3 cm^3). While the soltuion was being stirred, diphenyl phosphate (25 mg, 0.10 mmol), triethylamine (5 mg, 0.05 mmol), and iron(III) chloride hexahydrate (27 mg, 0.10 mmol) were added, and the resulting solution was filtered. The filtrate was left standing for several days at room temperature to give black crystals. They were collected by filtration and dried in vacuo over P_2O_5: Yield, 17 mg (14%). Found: C, 50.81; H, 3.25; N, 2.76%. Calcd for $C_{52}H_{40}Br_2Fe_2N_2O_{12}P_2$: C, 51.26; H, 3.31; N, 2.30%. IR (KBr, cm^{-1}) ν(C=N) 1618, ν(P–O) 1178, 1063. μ_{eff}(295 K) per molecule/B.M. 8.47. Diffuse reflectance spectrum: λ_{max}/nm 262, 319, 520. Electronic spectrum in dmf: λ_{max}/nm(ε per Fe/dm^3 mol^{-1} cm^{-1}) 295 (12300), 317sh (11300), 434sh (2380), 487 (3110).

$[Fe_2(L^b)_2(CH_3COCHCOCH_3)_2]$ (5). After 2-hydroxy-5-bromobenzylamine (20 mg, 0.099 mmol) and salicylaldehyde (12 mg, 0.098 mmol) were dissolved in acetonitrile (15 cm^3), iron(III) acetylacetonate (35 mg, 0.10 mmol) was added with stirring. After the solution had been filtered, the filtrate was left at room temperature for several days to give black crystals. Yield, 27 mg (29%). Found: C, 49.74; H, 3.73; N, 3.13%. Calcd for $C_{38}H_{34}Br_2Fe_2N_2O_8$: C, 49.71; H, 3.73; N, 3.05%. IR (KBr, cm^{-1}) ν(C=N) 1617; ν(C=C + C=O($acac^-$)) 1581; ν(C=C + C=O($acac^-$)) 1528. μ_{eff} (295 K) per molecule/B.M. 7.38. Diffuse reflectance spectrum: λ_{max}/nm 257, 319, 466. Electronic spectrum in dmf: λ_{max}/nm(ε per Fe/dm^3 mol^{-1} cm^{-1}) 310sh (13500), 430sh (3200), 477 (3900).

$[Fe_2(L^b)_2(CH_3CO_2)_2]$ (6). After 2-hydroxy-5-chlorobenzylamine (16 mg, 0.10 mmol) and salicylaldehyde (12 mg, 0.098 mmol) were dissolved in acetonitrile (10 cm^3), acetic acid (12 mg, 0.20 mmol), triethylamine (22 mg, 0.22 mmol), and iron(III) chloride hexahydrate (27 mg, 0.10 mmol) were added. After the solution had been filtered, the filtrate was allowed to stand for several days at room temperature. Black crystals resulted, which were filtered and dried in vacuo over P_2O_5: Yield, 21 mg (28%). Found: C, 51.37; H, 3,44; N, 3.74%. Calcd for $C_{32}H_{26}Cl_2Fe_2N_2O_8$: C, 51.30; H, 3.50; N, 3.74%. IR (KBr, cm^{-1}) ν(C=N) 1618, $\nu_{as}(COO^-)$ 1539, $\nu_s(COO^-)$ 1400. μ_{eff} (295 K) per molecule/B.M. 8.38. Diffuse reflectance spectrum: λ_{max}/nm 255, 315, 500. Electronic spectrum in dmf: λ_{max}/nm(ε per Fe/dm^3 mol^{-1} cm^{-1}) 292 (16900), 415 (4580), 450sh (4130).

$[Fe_2(L^c)_2(CH_3CO_2)_2]$ (7). This complex was prepared in the same way as that for **6**, except for using an equimolar amount of 2-hydroxybenzylamine instead of 2-hydroxy-5-chlorobenzylamine. Yield, 21 mg (31%). Found: C, 56.20; H, 4.18; N, 4.34%. Calcd for $C_{32}H_{28}Fe_2N_2O_8$: C, 56.50; H, 4.15; N, 4.12%. IR (KBr, cm^{-1}) ν(C=N) 1615; $\nu_{as}(COO^-)$ 1531, $\nu_s(COO-)$ 1400. μ_{eff}(295 K) per molecule/B.M. 8.69. Diffuse reflectance spectrum: λ_{max}/nm 250, 323, 506. Electronic spectrum in dmf: λ_{max}/nm(ε per Fe/dm^3 mol^{-1} cm^{-1}) 280sh (6250), 314sh (4630), 422 (1860), 452sh (1800).

Measurements. Carbon, hydrogen, and nitrogen analyses were carried out using a Perkin-Elmer 2400 Series II CHNS/O Analyzer. Infrared spectra were measured with a JASCO Infrared Spectrophotometer model IR700 in the 4000–400 cm^{-1} region on a KBr disk. The electronic spectra were measured with a Shimadzu UV-vis-NIR Recording Spectrophotometer Model UV-3100. The temperature dependence of magnetic susceptibilities was measured with a Quantum Design MPMS-5S SQUID susceptometer operating at a magnetic field of 0.5 T between 2 and 300 K. The field dependence of magnetization was measured up to 4.8 T at 4.5 K. The susceptibilities were corrected for the diamagnetism of the constituent atoms using Pascal's constants.[24] The effective magnetic moments were calculated from the equation $\mu_{eff} = 2.828\sqrt{\chi_m T}$, where χ_m is the magnetic susceptibility per mole.

X-ray Crystal Structure Analysis. The crystal data and details of the data collection are given in Table 1. The crystals were sealed in a glass capillary together with the mother liquor and mounted on an Enraf-Nonius CAD4 diffractometer, using graphite-monochromated Mo-$K\alpha$ radiation at 25 ± 1 °C. The unit-cell parameters were determined by a least-squares refinement based on 25 reflections with $20 \le 2\theta \le 30°$. Intensitiy data were corrected for Lorentz-polarization effects. The structures were solved by direct methods and refined by full-matrix least-squares methods. All of the non-hydrogen atoms were refined with anisotropic thermal parameters. The hydrogen atoms were inserted at their calculated positios and fixed at their positions. The final discrepancy factors, $R = \Sigma||F_o| - |F_c||/\Sigma|F_o|$, $R_w = [\Sigma w(|F_o| - |F_c|)^2/\Sigma w|F_o|^2]^{1/2}$, are listed in Table 1. The weighting scheme, $w = 1/[\sigma^2(|F_o|) + (0.02|F_o|)^2 + 1.0]$, was employed. All of the calculations were carried out on a Micro-VAXII computer using a Enraf–Nonius SDP program package.[25] The atomic coordinates and thermal parameters of the atoms and the anisotropic thermal parameters of the non-hydrogen atoms have been deposited as Document No. 74045 at the Office of the Editor of Bull. Chem. Soc. Jpn. Crystallographic data have been deposited at the CCDC, 12

Table 1. Crystal Data and Data Collection Details

Complex	$[Fe_2(L^a)_2(CH_3CO_2)_2]\cdot 2CH_3CN$(**1**·2$CH_3CN$)	$[Fe_2(L^a)_2(C_6H_5CO_2)_2]$ (**2**)	$[Fe_2(L^a)_2\{(CH_3)_3C\text{-}CO_2\}_2]$ (**3**)	$[Fe_2(L^a)_2\{(C_6H_5O_2)_2PO_2\}_2]\cdot 4CH_3CN$(**4**·4$CH_3CN$)	$[Fe_2(L^a)_2(CH_3CO\text{-}CHCOCH_3)]$ (**5**)	$[Fe_2(L^b)_2\{(CH_3CO_2)_2\}]\cdot 2CH_3CN$(**6**·2$CH_3CN$)	$[Fe_2(L^c)_2(CH_3CO_2)_2]$ (**7**)
Formula	$C_{36}H_{32}Br_2Fe_2N_4O_8$	$C_{42}H_{30}Br_2Fe_2N_2O_8$	$C_{38}H_{38}Br_2Fe_2N_2O_8$	$C_{60}H_{52}Br_2Fe_2N_6O_{12}P_2$	$C_{38}H_{34}Br_2Fe_2N_2O_8$	$C_{36}H_{32}Cl_2Fe_2N_4O_8$	$C_{32}H_{28}Fe_2N_2O_8$
F.W.	920.1	962.2	922.2	1382.6	918.2	831.3	680.3
Crystal system	triclinic	monoclinic	orthorhombic	triclinic	triclinic	triclinic	monoclinic
Space group	$P\bar{1}$	$P2_1/c$	*Pbca*	$P\bar{1}$	$P\bar{1}$	$P\bar{1}$	$P2_1/n$
a/Å	10.703(4)	12.202(15)	10.371(3)	11.363(2)	12.079(7)	10.673(5)	12.043(6)
b/Å	11.310(5)	10.829(2)	22.038(6)	15.183(2)	14.229(19)	11.301(5)	7.683(2)
c/Å	8.584(4)	15.869(18)	17.005(7)	10.243(2)	11.397(9)	8.545(4)	16.410(8)
α/°	96.08(3)			92.68(1)	94.16(5)	95.89(3)	
β/°	102.78(2)	110.84(6)		116.56(1)	96.22(4)	103.43(3)	109.72(2)
γ/°	108.95(2)			107.48(1)	89.96(5)	108.88(2)	
V/Å^3	940.4(7)	1959.7(34)	3886.5(22)	1473.3(5)	1942.1(32)	930.6(8)	1421.0(11)
Z	1	2	4	1	2	1	2
D_c/g cm^{-3}	1.63	1.63	1.58	1.56	1.57	1.48	1.59
D_m/g cm^{-3}	1.62	1.62	1.56	1.56	1.56	1.49	1.58
μ(Mo $K\alpha$)/cm^{-1}	29.29	28.13	28.33	19.53	28.35	9.77	10.75
Crystal size/mm	0.45 × 0.20 × 0.12	0.70 × 0.50 × 0.07	0.40 × 0.40 × 0.05	0.30 × 0.20 × 0.05	0.38 × 0.45 × 0.08	0.40 × 0.20 × 0.12	0.60 × 0.55 × 0.15
2θ range/°	2.0–48.0	2.0–48.0	2.0–48.0	2.0–48.0	2.0–48.0	2.0–49.0	2.0–50.0
Total no. of reflections measured	2949	3265	3453	4612	6069	3082	2699
No. of unique reflections with $I \geq 3\,\sigma(I)$	2198	1997	1038	2347	3401	2284	2022
R	0.032	0.062	0.061	0.044	0.042	0.039	0.037
R_w	0.035	0.078	0.067	0.048	0.045	0.042	0.045

Union Road, Cambridge CB2, 1EZ, UK and copies can be obtained on request, free of charge, by quoting the publication citation and the deposition numbers 163629–163635.

Results and Discussion

Complexes **1**–**7** were prepared via one-pot synthesis, given in the Experimental Section. In previous papers, we described the synthesis and characterization of other related metal complexes with the present Schiff-base ligands. The Schiff-base ligands afforded mononuclear Mn(IV) species, $[Mn(L)_2]$ (H_2L = H_2L^a, H_2L^b, and H_2L^c);[19] mononuclear V(IV) species, $[VO(HL^c)_2]$; and dinuclear V(V) species, $[(VO)_2(L^c)_2O]$,[20] stabilizing such a higher oxidation state owing to the presence of the two phenolic-oxygen donors. In the present cases, the reaction of the Schiff-base ligands with iron(III) in the presence of exogenous ligands gave black crystals of dinuclear Fe(III) species, which have the general composition $[Fe_2L_2X_2]\cdot n CH_3CN$ (L = L^a, L^b, and L^c; X = $CH_3CO_2^-$, $C_6H_5CO_2^-$, $(CH_3)_3CCO_2^-$, $(C_6H_5O)_2PO_2^-$, and $CH_3COCHCOCH_3^-$; n = 0, 2, and 4). This is in contrast with the cases for the manganese and vanadium systems, and is probably due to the unstable property of the Fe(IV) state. Similarly, we could isolate dinuclear Cu(II) species, $[Cu_2(L)_2(dmso)_2]$ (H_2L = H_2L^a and H_2L^b, dmso = dimethyl sulfoxide) for copper systems by using the same Schiff-base ligands (Scheme 1).[21]

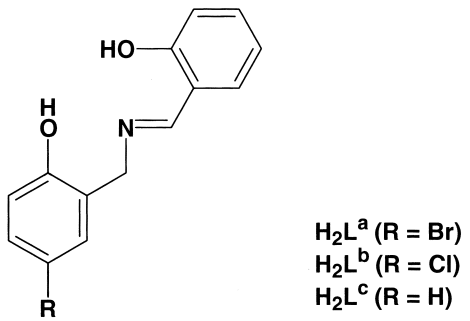

Scheme 1.

The X-ray crystallography of **1** reveals a dinuclear structure where two iron(III) ions are doubly bridged by phenoxo-oxygen atoms of the Schiff-base ligands, L^a. A perspective view of the molecule is shown in Fig. 1. Selected bond distances and angles are listed in Table 2. Only a few examples of strcturally characterized Fe(III) complexes with di-μ-phenoxo-oxygen-bridging are known.[16] The dinuclear molecule is centrosymmetric with a crystallographic inversion center in the middle of the Fe_2O_2 core. The two iron atoms are further bridged by two acetate bridging in a *syn–syn* configuration. The antisymmetric and symmetric C–O stretching bands of the acetate ions were found at 1530 and 1400 cm^{-1}, respectively. This feature is in harmony with the *syn–syn* bridging mode of the acetate group.[26] The unique bridging mode of the two acetate ions was already found in $[Mn_2(spa)_2(CH_3CO_2)_2]$ (H_2spa = 3-salicylideneamino-1-propanol).[27] Each iron atom (Fe) is coordinated to two phenoxo-oxygen and one imino-nitrogen atoms (O1, O2, and N1) of the Schiff-base ligand L^a and one

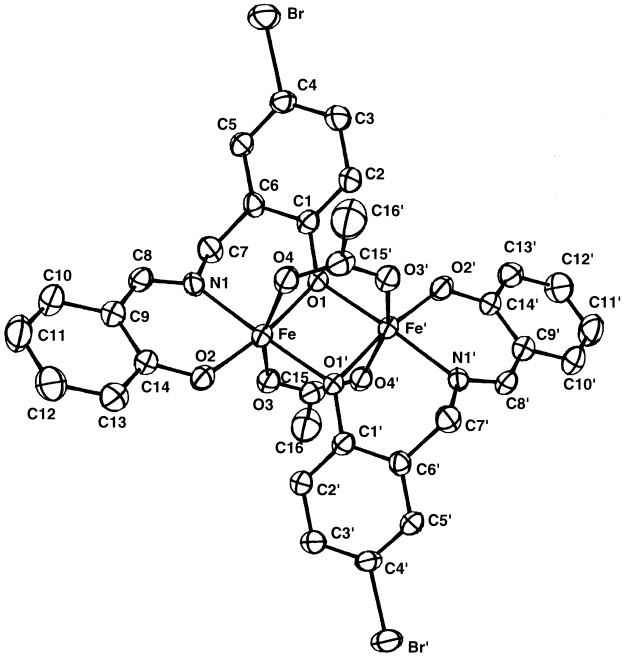

Fig. 1. ORTEP drawing of the structure of $[Fe_2(L^a)_2(CH_3CO_2)_2]\cdot 2CH_3CN$ (**1**$\cdot 2CH_3CN$) showing the 50% probability thermal ellipsoids and atom labeling scheme. Hydrogen atoms and solvent molecules are omitted for clarity. Primed and unprimed atoms are related by the inversion.

phenoxo-oxygen atom (O1′) of the other ligand L^a. The fifth and sixth coordination sites are occupied by the two acetato oxygen atom (O3 and O4). The iron centers are arranged in an approximate octahedral geometry with distances of Fe–O1 2.107(3), Fe–O1′ 2.021(3), Fe–O2 1.885(3), Fe–O3 2.039(2), Fe–O4 2.055(3), Fe–N 2.083(4) Å. The Fe–Fe separation and Fe–O–Fe angle are 2.957(1) Å and 91.5(1)°, respectively. These values are significantly smaller than those yet found for complexes with the $Fe^{III}_2(OR)_2$ complexes [di-μ-hydroxo-bridged Fe^{III}_2 complexes:[14] Fe–Fe 3.078(2)–3.155(3) Å, Fe–O–Fe 100.7(4)–105.3(4)°; di-μ-alkoxo-bridged Fe^{III}_2 complexes:[15] Fe–Fe 3.049(3)–3.21(1) Å, Fe–O–Fe 101.8(3)–107.4(6)°; di-μ-phenoxo-bridged Fe^{III}_2 complexes:[16] Fe–Fe 3.06–3.186(4) Å, Fe–O–Fe 97.06(9)–105.64(3)°].

The crystal structures of **2** and **3** consist of similar centrosymmetric dinuclear molecules to that of **1**, as shown in Figs. 2 and 3, respectively. The two Fe atoms are bridged by two phenoxo-oxygen atoms of L^a to form an equatorial coplane. The carboxylate groups of benzoate and pivalate ions are positioned above and below the equatorial plane containing the Schiff-base moiety, and is involved in the bridges in a *syn–syn* configuration. The Fe–Fe separation and Fe–O–Fe angle for **2** and **3** are 2.953(2) Å and 91.6(2)° and 2.959(3) Å and 92.3 (4)°, respectively; these values are significantly smaller than those for the reported $Fe^{III}_2(OR)_2$ complexes.[14–16]

The crystal structure of **4** is shown in Fig. 4. The molecule is crystallographically centrosymmetric. The two Fe atoms are bridged by two phenoxo-oxygen atoms of the Schiff-base ligands L^a. The Fe atoms are further bridged by two diphenyl phosphate ions with a similar triatomic bridging mode to the *syn–syn* acetate bridge. The Fe–Fe distance and the Fe–O–Fe

Table 2. Selected Bond distances (Å) and Angles (°) of with Their Estimated Standard Deviations in Parentheses

$[Fe_2(L^a)_2(CH_3CO_2)_2]\cdot 2CH_3CN$ (**1**·2CH$_3$CN)			
Fe–Fe′[a]	2.957(1)	Fe–O3	2.039(2)
Fe–O1	2.107(3)	Fe–O4	2.055(3)
Fe–O1′	2.021(3)	Fe–N1	2.083(4)
Fe–O2	1.885(3)		
O1–Fe–O1′	88.5(1)	O1′–Fe–N1	173.9(1)
O1–Fe–O2	172.3(1)	O2–Fe–O3	103.2(1)
O1–Fe–O3	82.0(1)	O2–Fe–O4	94.5(1)
O1–Fe–O4	81.5(1)	O2–Fe–N1	88.1(1)
O1–Fe–N1	86.0(1)	O3–Fe–O4	160.0(1)
O1′–Fe–O2	97.6(1)	O3–Fe–N1	91.5(1)
O1′–Fe–O3	85.1(1)	O4–Fe–N1	98.4(1)
O1′–Fe–O4	83.4(1)	Fe–O1–Fe′	91.5(1)
$[Fe_2(L^a)_2(C_6H_5CO_2)_2]$ (**2**)			
Fe–Fe′[a]	2.953(2)	Fe–O3	2.044(8)
Fe–O1	2.081(6)	Fe–O4	2.055(8)
Fe–O1′	2.037(6)	Fe–N	2.089(7)
Fe–O2	1.875(7)		
O1–Fe–O1′	88.4(2)	O1′–Fe–N	174.5(3)
O1–Fe–O2	173.8(3)	O2–Fe–O3	100.1(3)
O1–Fe–O3	83.8(3)	O2–Fe–O4	95.9(3)
O1–Fe–O4	81.3(3)	O2–Fe–N	88.6(3)
O1–Fe–N1	86.1(3)	O3–Fe–O4	160.9(3)
O1′–Fe–O2	96.9(3)	O3–Fe–N	95.5(3)
O1′–Fe–O3	83.4(3)	O4–Fe–N	95.2(3)
O1′–Fe–O4	84.5(3)	Fe–O1–Fe′	91.6(2)
$[Fe_2(L^a)_2\{(CH_3)_3CCO_2\}_2]$ (**3**)			
Fe–Fe′[b]	2.959(3)	Fe–O3	2.014(11)
Fe–O1	2.079(10)	Fe–O4	2.061(10)
Fe–O1′	2.024(10)	Fe–N	2.095(13)
Fe–O2	1.873(11)		
O1–Fe–O1′	87.7(4)	O1′–Fe–N	173.6(4)
O1–Fe–O2	174.0(5)	O2–Fe–O3	100.2(5)
O1–Fe–O3	81.4(4)	O2–Fe–O4	96.9(5)
O1–Fe–O4	82.6(4)	O2–Fe–N	87.7(5)
O1–Fe–N	86.4(4)	O3–Fe–O4	160.4(5)
O1′–Fe–O2	98.2(5)	O3–Fe–N	91.6(5)
O1′–Fe–O3	85.0(4)	O4–Fe–N	98.7(5)
O1′–Fe–O4	83.0(4)	Fe–O1–Fe′	92.3(4)
$[Fe_2(L^a)_2\{(C_6H_5O)_2PO_2\}_2]\cdot 4CH_3CN$(**4**·4CH$_3$CN)			
Fe–Fe′[c]	3.091(1)	Fe–O3	2.029(5)
Fe–O1	2.115(5)	Fe–O4	2.047(5)
Fe–O1′	2.030(4)	Fe–N1	2.076(6)
Fe–O2	1.877(5)		
O1–Fe–O1′	83.6(2)	O1′–Fe–N1	170.8(2)
O1–Fe–O2	174.8(2)	O2–Fe–O3	99.8(2)
O1–Fe–O3	83.8(2)	O2–Fe–O4	93.2(2)
O1–Fe–O4	83.7(2)	O2–Fe–N1	88.9(2)
O1–Fe–N1	87.3(2)	O3–Fe–O4	165.3(2)
O1′–Fe–O2	100.3(2)	O3–Fe–N1	92.1(2)
O1′–Fe–O3	86.0(2)	O4–Fe–N1	95.0(2)
O1′–Fe–O4	85.0(2)	Fe–O1–Fe′	96.4(2)
$[Fe_2(L^a)_2(CH_3COCHCOCH_3)_2]$ (**5**)			
FeA–FeA′[d]	3.270(1)	FeB–FeB″[e]	3.275(1)
FeA–O1A	2.036(4)	FeB–O1B	2.043(5)
FeA–O1A′	2.051(4)	FeB–O1B″	2.051(4)
FeA–O2A	1.901(4)	FeB–O2B	1.888(5)
FeA–O3A	1.998(5)	FeB–O3B	2.013(5)
FeA–O4A	2.010(4)	FeB–O4B	2.019(5)
FeA–NA	2.149(6)	FeB–NB	2.133(5)
O1A–FeA–O1A′	73.7(2)	O1B–FeB–O1B″	73.8(2)
O1A–FeA–O2A	165.2(2)	O1B–FeB–O2B	164.7(2)
O1A–FeA–O3A	96.9(2)	O1B–FeB–O3B	96.9(2)
O1A–FeA–O4A	91.8(2)	O1B–FeB–O4B	90.7(2)
O1A–FeA–NA	83.5(2)	O1B–FeB–NB	84.4(2)
O1A′–FeA–O2A	95.7(2)	O1B″–FeB–O2B	94.1(2)
O1A′–FeA–O3A	91.8(2)	O1B″–FeB–O3B	91.4(2)
O1A′–FeA–O4A	165.0(2)	O1B″–FeB–O4B	163.6(2)
O1A′–FeA–NA	96.7(2)	O1B″–FeB–NB	98.6(2)
O2A–FeA–O3A	93.6(2)	O2B–FeB–O3B	92.4(2)
O2A–FeA–O4A	99.3(2)	O2B–FeB–O4B	102.1(2)
O2A–FeA–NA	87.8(2)	O2B–FeB–NB	88.5(2)
O3A–FeA–O4A	86.1(2)	O3B–FeB–O4B	85.1(2)
O3A–FeA–NA	171.3(2)	O3B–FeB–NB	169.9(2)
O4A–FeA–NA	85.2(2)	O4B–FeB–NB	84.8(2)
FeA–O1A–FeA′	106.3(2)	FeB–O1B–FeB″	106.2(2)
$[Fe_2(L^b)_2\{(CH_3CO_2)_2\}]\cdot 2CH_3CN$ (**6**·2CH$_3$CN)			
Fe–Fe′[f]	2.960(1)	Fe–O3	2.037(2)
Fe–O1	2.103(3)	Fe–O4	2.053(2)
Fe–O1′	2.021(3)	Fe–N1	2.089(4)
Fe–O2	1.883(3)		
O1–Fe–O1′	88.3(1)	O1′–Fe–N1	173.7(1)
O1–Fe–O2	172.3(1)	O2–Fe–O3	103.3(1)
O1–Fe–O3	81.6(1)	O2–Fe–O4	94.6(1)
O1–Fe–O4	81.7(1)	O2–Fe–N1	87.8(1)
O1–Fe–N1	86.1(1)	O3–Fe–O4	159.8(1)
O1′–Fe–O2	98.1(1)	O3–Fe–N1	91.5(1)
O1′–Fe–O3	84.9(1)	O4–Fe–N1	98.7(1)
O1′–Fe–O4	83.3(1)	Fe–O1–Fe′	91.7(1)
$[Fe_2(L^c)_2(CH_3CO_2)_2]$ (**7**)			
Fe–Fe[a]	2.930(1)	Fe–O3	2.060(3)
Fe–O1	2.093(3)	Fe–O4	2.053(3)
Fe–O1′	2.017(2)	Fe–N	2.106(3)
Fe–O2	1.877(3)		
O1–Fe–O1′	89.1(1)	O1′–Fe–N	171.8(1)
O1–Fe–O2	173.9(1)	O2–Fe–O3	100.4(1)
O1–Fe–O3	81.9(1)	O2–Fe–O4	97.0(1)
O1–Fe–O4	81.6(1)	O2–Fe–N	88.2(1)
O1–Fe–N	86.3(1)	O3–Fe–O4	160.5(1)
O1′–Fe–O2	96.7(1)	O3–Fe–N	87.8(1)
O1′–Fe–O3	84.8(1)	O4–Fe–N	101.4(1)
O1′–Fe–O4	84.6(1)	Fe–O1–Fe′	90.9(1)

a) Prime refers to the equivalent position (1−x, −y, −z). b) Prime refers to the equivalent position (2−x, 1−y, 1−z). c) Prime refers to the equivalent position (1−x, 1−y, 1−z). d) Prime refers to the equivalent position (1−x, 1−y, −z). e) Double prime refers to the equivalent position (2−x, −y, 2−z). f) Prime refers to the equivalent position (1−x, −y, 1−z).

angle are 3.091(1) Å and 96.4(2)°, respectively. The elongation of the Fe–Fe distance and the obtuse Fe–O–Fe angle compared with those of **1**–**3** may be caused by the bigger triatomic bridging groups. The coordination geometry of each iron atom is a distorted octahedral with Fe–O1 (2.115(5) Å), Fe–O2 (1.877(5) Å), Fe–O3 (2.029(5) Å), Fe–O4′ (2.047(5) Å), Fe–O1′ (2.030(4) Å), and Fe–N1 (2.076(6) Å).

The crystal of **5** contains two crystallographically independent dinuclear molecules; they are abbreviated as A and B. Figure 5 shows the structure of molecule A. Both comprise a

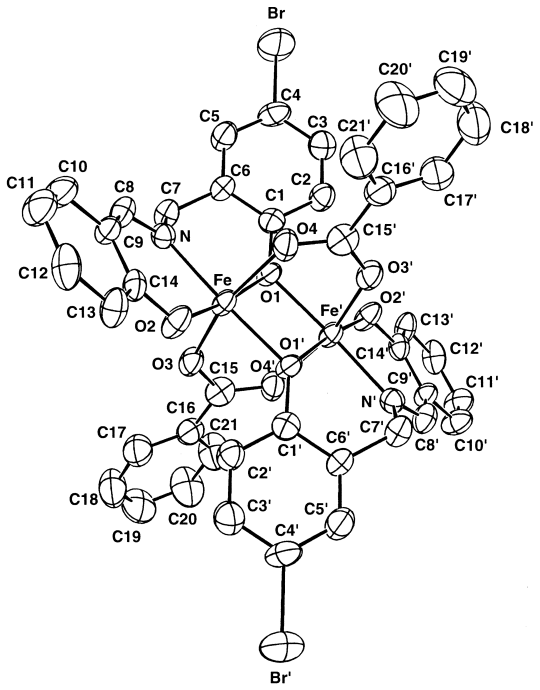

Fig. 2. ORTEP drawing of the structure of $[Fe_2(L^a)_2(C_6H_5CO_2)_2]$ (**2**) showing the 50% probability thermal ellipsoids and atom labeling scheme. Hydrogen atoms are omitted for clarity. Primed and unprimed atoms are related by the inversion.

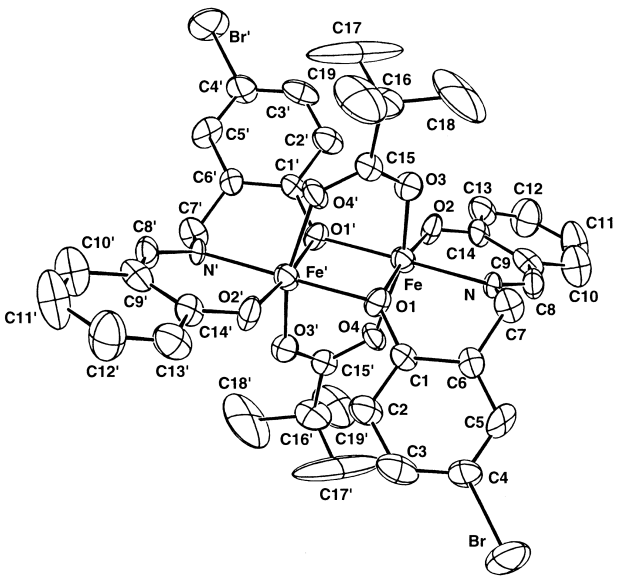

Fig. 3. ORTEP drawing of the structure of $[Fe_2(L^a)_2\{(CH_3)_3CCO_2\}_2]$ (**3**) showing the 50% probability thermal ellipsoids and atom labeling scheme. Hydrogen atoms and solvent molecules are omitted for clarity. Primed and unprimed atoms are related by the inversion.

similar centrosymmetric dinuclear molecule. In the complex, the two iron atoms are bridged by only phenoxo-oxygen atoms of the Schiff-base ligands. The acetylacetonato group is coordinated to each iron atom in a didentate fashion to occupy the

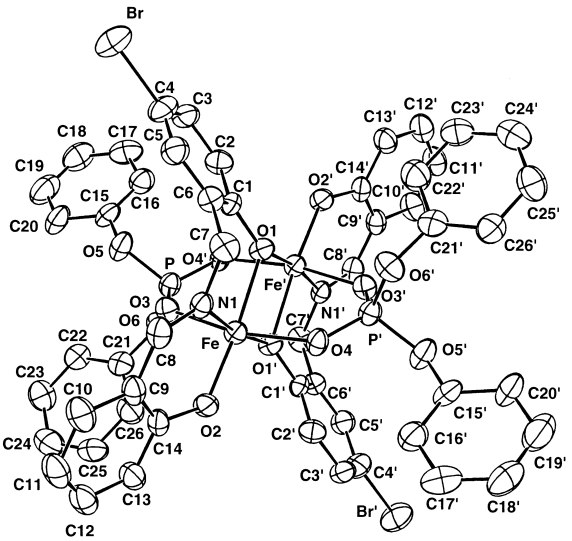

Fig. 4. ORTEP drawing of the structure of $[Fe_2(L^a)_2\{(C_6H_5O)_2PO_2\}_2]\cdot 4CH_3CN$ (**4**·4CH_3CN) showing the 50% probability thermal ellipsoids and atom labeling scheme. Hydrogen atoms and solvent molecules are omitted for clarity. Primed and unprimed atoms are related by the inversion.

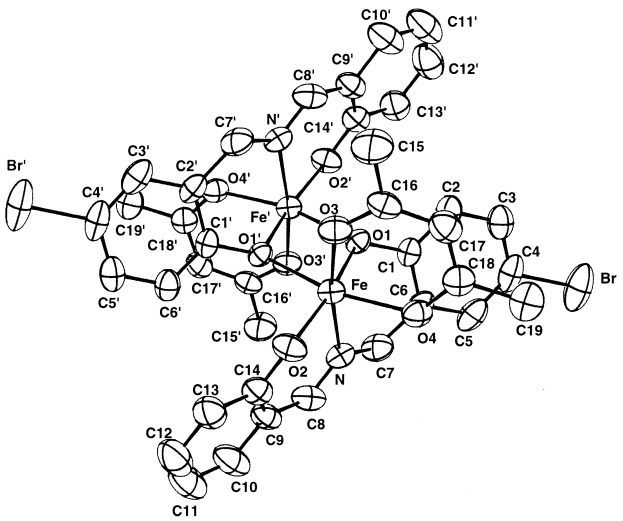

Fig. 5. ORTEP drawing of the structure (molecule A) of $[Fe_2(L^a)_2(CH_3COCHCOCH_3)_2]$ (**5**) showing the 50% probability thermal ellipsoids and atom labeling scheme. Hydrogen atoms are omitted for clarity. Primed and unprimed atoms are related by the inversion.

axial and equatorial positions of the distorted octahedral geometry. No significant difference in the geometries of the two dinuclear molecules can be recognized between A and B. The Fe–Fe separation and Fe–O–Fe angle are 3.270(1) Å and 106.3(2)° for A and 3.275(1) Å and 106.2(2)° for B, respectively. These values are much larger than those of **1**–**4** and comparable to those of the usual $Fe^{III}_2(OR)_2$ complexes.[14,15,16b]

As shown in Figs. 6 and 7, the molecular structures of **6** and **7** are very similar to that of **1**. The two Fe atoms are bridged by two phenoxo-oxygen atoms of the Schiff-base ligands L^b or L^c and two acetate ions. The Fe–Fe sepapration and Fe–O–Fe

angle for **6** and **7** are 2.960(1) Å and 91.7(1)° and 2.930(1) Å and 90.9(1)°, respectively.

For the di-μ-phenoxo-di-μ-carboxylato-bridged complexes, **1**–**3**, **6**, **7**, the Fe–O–Fe angle varies from 90.9(1) to 92.3(4)° and the Fe–Fe separation from 2.930(1) to 2.960(1) Å; for the di-μ-phenoxo-di-μ-phosphato-bridged complex **4**, the Fe–O–Fe angle is 96.4(2)° and the Fe–Fe separation is 3.091(1) Å. The Fe–O–Fe angles for the di-μ-phenoxo-bridged complex **5** are 106.3(2) and 106.2(2)° and the Fe–Fe separations are 3.270(1) and 3.275(1) Å, respectively. These facts show that the short Fe–Fe separation and small Fe–O–Fe angle in the di-μ-phenoxo-di-μ-carboxylato-bridged complexes may be due to constraints imposed by the incorporation of bridging carboxylate groups.

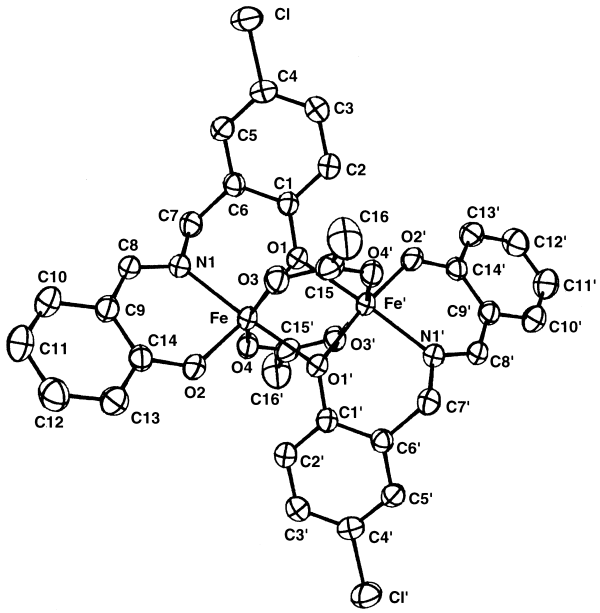

Fig. 6. ORTEP drawing of the structure of $[Fe_2(L^b)_2(CH_3CO_2)_2]\cdot 2CH_3CN$ (**6**·2CH_3CN) showing the 50% probability thermal ellipsoids and atom labeling scheme. Hydrogen atoms and solvent molecules are omitted for clarity. Primed and unprimed atoms are related by the inversion.

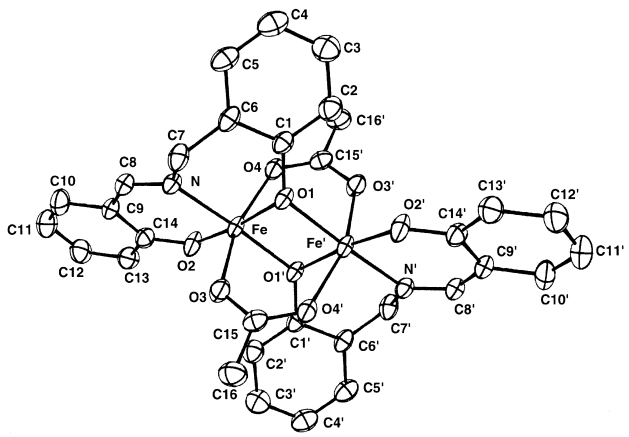

Fig. 7. ORTEP drawing of the structure of $[Fe_2(L^c)_2(CH_3CO_2)_2]$ (**7**) showing the 50% probability thermal ellipsoids and atom labeling scheme. Hydrogen atoms are omitted for clarity. Primed and unprimed atoms are related by the inversion.

The diffuse reflectance spectra of the present complexes are similar, and are characterized by intense absorptions around 255, 320 and 510 nm. The diffuse reflectance spectrum of **1** is shown in Fig. 8 as a representative example. Since all d–d transitions are expected to be spin forbidden, the observed absorptions are most likely to arise from charge-transfer transitions and/or intraligand transitions. Especially, the band around 510 nm can be assigned as a charge-transfer transition from bridging phenoxo-oxygen to iron(III). For the present di-μ-phenoxo-bridged iron(III) dimers, there is no evidence for a substantial intensity enhancement of the spin-forbidden d–d bands, such as that found in certain oxo-bridged iron(III) dimers.[28] The absorption spectra in dmf for the complexes are in generally agreement with the solid-state spectra. All complexes show a shoulder at 450–487 nm, followed by two strong absorptions beginning at about 420 nm up to the peak maximum at about 290 nm. The large values of the molar extinction coefficient of these absorptions indicates that these may be due to ligand to iron(III) charge-transfer bands. The higher energy band at around 290 nm may be assigned as ligand $\pi\rightarrow\pi^*$ transitions.

The room-temperature magnetic moments of these complexes [**1**, 8.64 B.M. (295 K); **2**, 8.34 B.M. (295 K); **3**, 8.37 B.M. (295 K); **4**, 8.47 B.M. (295 K); **5**, 7.32 B.M. (295 K); **6**, 8.38 B.M. (295 K); **7**, 8.69 B.M. (295 K)] are close to the spin-only value (8.37 B.M.) for non-interacting two high-spin d^5 ions, except for **5**. The high-spin character of the present iron(III) complexes is in harmony with the electronic spectra. The magnetic moment of **5** is considerably lower than those of the usual high-spin Fe(III) complexes, suggesting an antiferromagnetic behavior of this complex. The magnetic susuceptibilities were measured over the temperature range 2–300 K. As expected, **5** is antiferromagnetic, since the magnetic moment decreases with lowering the temperature (Fig. 9). On the other hand, the profiles of the temperature dependence of the magnetic moments of the other complexes, **1**–**3**, **5**–**7**, show that a ferromagnetic interaction is operative, as illustrated in Figs.

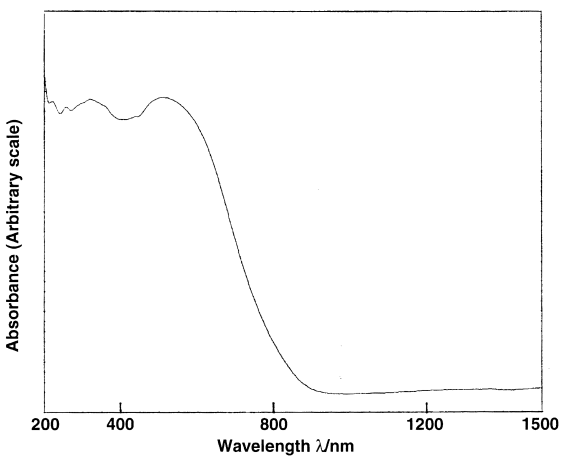

Fig. 8. Diffuse reflectance spectrum of $[Fe_2(L^a)_2(CH_3CO_2)_2]$ (**1**).

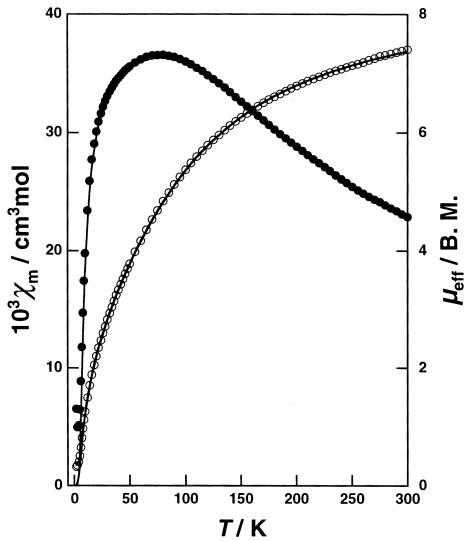

Fig. 9. Magnetic susceptibity data (●) and effective magnetic moments (○) of $[Fe_2(L^a)_2(CH_3COCHCOCH_3)_2]$ (**5**).

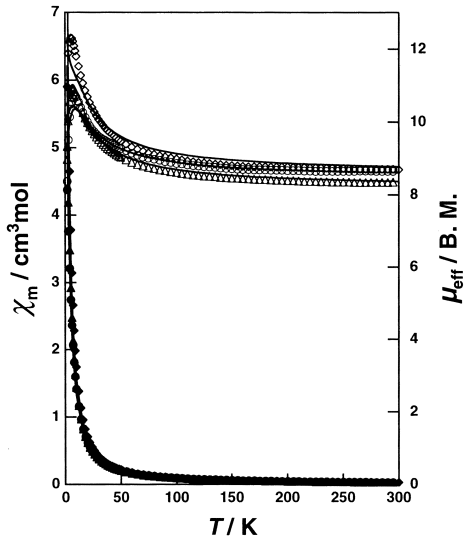

Fig. 10. Magnetic susceptibity data and effective magnetic moments of $[Fe_2(L^a)_2(CH_3CO_2)_2]$ (**1**) (●, ○), $[Fe_2(L^a)_2(C_6H_5CO_2)_2]$ (**2**) (▲, △) and $[Fe_2(L^c)_2(CH_3CO_2)_2]$ (**7**) (◆, ◇).

10 and 11. In the case of **4**, the magnetic moment is almost constant from 30 to 300 K, as shown in Fig. 11, indicating that the magnetic interaction between the metal ions is small. The magnetic-susceptibility data were analyzed with the Van Vleck equation based on the Heisenberg model ($H = -2JS_1 \cdot S_2$ ($S_1 = S_2 = 5/2$)):

$\chi_m = Ng^2\beta^2/k(T - \theta)(2e^{2x} + 10e^{6x} + 28e^{12x} + 60e^{20x} + 110e^{30x})/(1 + 3e^{2x} + 5e^{6x} + 7e^{12x} + 9e^{20x} + 11e^{30x})$,

where $x = J/kT$ and the other symbols have their usual meanings.

The values for the three independent parameters (g, J, and θ) determined by the fitting procedure are listed in Table 3. The small values of θ suggest that second-order effects, such as intermolecular interaction and zero-field splitting, are weak.

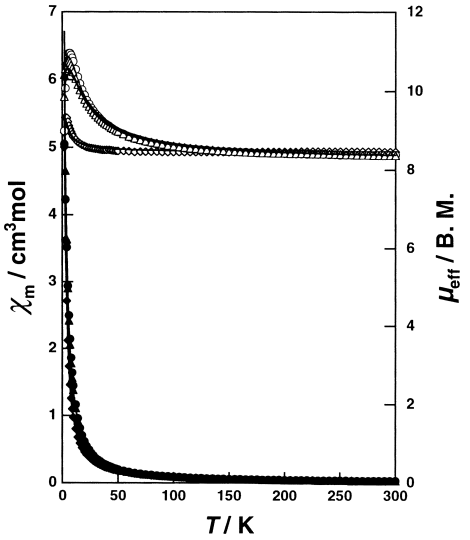

Fig. 11. Magnetic susceptibity data and effective magnetic moments of $[Fe_2(L^a)_2\{(CH_3)_3CCO_2\}_2]$ (**3**) (▲, △), $[Fe_2(L^a)_2\{(C_6H_5O)_2PO_2\}_2]$ (**4**) (◆, ◇), and $[Fe_2(L^b)_2(CH_3CO_2)_2]$ (**6**) (●, ○).

The J values for the present di-μ-phenoxo-bridged complexes range from $-9.24(6)$ cm^{-1} for the acetylacetonate complex **5** to 1.56(15) cm^{-1} for the acetate complex **7**. Complexes **1**–**4**, **6**, and **7** exhibit ferromagnetic coupling with J values of 0.17(5) to 1.56(15) cm^{-1}, while **5** exhibits an antiferromagnetic behavior with a J value of $-9.24(6)$ cm^{-1}. To confirm the ferromagnetic or antiferromagnetic nature of the ground state, the field dependence of the magnetization M at 4.5 K was measured. In Fig. 12, the experimental values of M are compared to the calculated curve of the Brillouin functions for an $S = 5$ state. For any value of the field, the experimental magnetization of **1**–**4**, **6** and **7** is larger than that for an isolated $S = 5/2$ state, and close to the value expected for an $S = 5$ spin state. On the other hand, the magnetization data of **5** show an $S = 0$ ground state.

A comparison of these complexes with related complexes provides some insight into the factors that affect the magnetic coupling interaction. The J value ($-9.24(6)$ cm^{-1}) obtained for **5** implies a much weaker coupling than those usually observed for singly bridged μ-oxo-diiron(III) compounds, which exhibit J values of -80 to -190 cm^{-1},[5] and is significantly smaller than those typically found for μ-oxo-μ-carboxylato-, μ-oxo-bis(μ-carboxylato)-, μ-oxo-μ-carbonato-, μ-oxo-di-μ-carbonato-, μ-oxo-μ-molybdato-, μ-oxo-μ-phosphato-, and μ-oxo-μ-phosphinato-diiron(III) complexes ($J = -83$–134 cm^{-1}).[7–13] In the case of the di-μ-oxo-bridged complex, a J value of -27 cm^{-1} was found.[6] Studies of several di-μ-hydroxo- and di-μ-alkoxo-bridged dinuclear iron(III) complexes also have been reported. The J values in these complexes range from -5.5 to -11.7 cm^{-1} and -6.5 to -28.6 cm^{-1}, respectively.[14,15] The strength of the antiferromagnetic interactions through the oxygen bridge is dependent on the nature of the bridge, the exchange for μ-oxo-bridged complexes being much stronger than for μ-hydroxo- or μ-alkoxo-bridged complexes. The values of the exchange integral of the present antiferromagnetic complex **5** is comparable to those of μ-hydroxo or μ-alkoxo-bridged dinuclear iron(III) systems. It is clear that

Table 3. Structural and Magnetic Data of Di-μ-Phenoxo-Bridged Dinuclear Iron(III) Complexes

Complex	Fe–O–Fe/°	Fe···Fe/Å	J/cm^{-1}	g	θ/K	Ref.
$[Fe_2(L^c)_2(CH_3CO_2)_2]$ (**7**)	90.9(1)	2.930(1)	1.56(15)	2.05(2)	0.33(7)	This work
$[Fe_2(L^a)_2(CH_3CO_2)_2]$ (**1**)	91.5(1)	2.957(1)	1.40(13)	2.02(2)	−0.92(11)	This work
$[Fe_2(L^a)_2(C_6H_5CO_2)_2]$ (**2**)	91.6(2)	2.953(2)	1.53(1)	1.96(1)	−0.32(1)	This work
$[Fe_2(L^b)_2\{(CH_3CO_2)_2\}$(**6**)	91.7(1)	2.960(1)	1.34(1)	1.97(1)	−0.33(6)	This work
$[Fe_2(L^a)_2\{(CH_3)_3CCO_2\}_2]$ (**3**)	92.3(4)	2.959(3)	1.23(4)	1.97(1)	−0.17(3)	This work
$[Fe_2(L^a)_2\{(C_6H_5O_2)_2PO_2\}_2]$ (**4**)	96.4(2)	3.091(1)	0.17(5)	2.02(2)	−0.49(4)	This work
$[Fe_2(salmp)_2]$	97.06(9)	3.063	1.21			16a
$[Fe_2(chphn)_2Cl_2]$	105.64(4)	3.186(4)	−10.9			16b
$[Fe_2(L^a)_2(CH_3COCHCOCH_3)_2]$ (**5**)	106.3(2), 106.2(2)	3.270(1), 3.275(1)	−9.24(6)	2.04(1)	−0.21(6)	This work

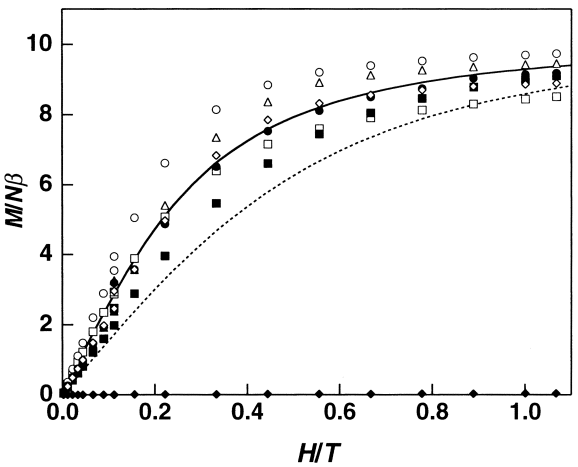

Fig. 12. Field dependence of the magnetization: experimental data for $[Fe_2(L^a)_2(CH_3CO_2)_2]$ (**1**) (△), $[Fe_2(L^a)_2(C_6H_5CO_2)_2]$ (**2**) (●), $[Fe_2(L^a)_2\{(CH_3)_3CCO_2\}_2]$ (**3**) (□), $[Fe_2(L^a)_2\{(C_6H_5O)_2PO_2\}_2]$ (**4**) (■), and $[Fe_2(L^a)_2(CH_3COCHCOCH_3)_2]$ (**5**) (◆), $[Fe_2(L^b)_2(CH_3CO_2)_2]$ (**6**) (◇), and $[Fe_2(L^c)_2(CH_3CO_2)_2]$ (**7**) (○); theoretical curves for an S = 5 spin state (g = 2.0) (—) and a non-interacting spin state (S = 5/2 + S = 5/2) (---).

the strength of the ferromagnetic coupling between the iron centers in a di-μ-phenoxo-di-μ-carboxylato diiron(III) unit is not significantly affected by the substituent group on the Schiff-base ligand nor the carboxylate bridges: J = 1.23(4)–1.56(15) cm^{-1} for **1**–**3**, **6**, and **7**. Although the superexchange pathways within the diiron(III) core consist of various orbital overlaps, the exchange interaction via the phenoxo-bridges should be important because of the monatomic bridges. In these complexes, the Fe–O–Fe angles are close to 90° and may be a major factor of the observed ferromagnetic coupling, since interactions of magnetic orbitals with orthogonal bridges will promote a ferromagnetic behavior. The substitution of carboxylate with diphenyl phosphate, however, weakens the ferromagnetic interaction in **4** to J = 0.17(5) cm^{-1}. The diphenyl phosphate substitution in the di-μ-phenoxo-di-μ-carboxylato complexes results in a slight elongation of the Fe–Fe distance and an increasing Fe–O–Fe angle [96.4(2)°], which might cancel the ferromagnetic coupling to some extent by causing an antiferromagnetic interaction between the Fe centers. Only two examples of complexes containing di-μ-phenoxo-diiron(III) cores have been previously reported, namely, $[Fe_2(salmp)_2]$·2dmf (H_2salmp = 2-bis(salicylideneamino)methylphenol)[16a] and $[Fe_2(chphn)_2Cl_2]$ (H_2chphn = *N*-(4-chloro-2-hydroxyphenyl)-3-hydroxy-2-naphthaldimine),[16b] where J = 1.21 cm^{-1} and Fe–O–Fe angle of 97.06(9)° and J = −10.9 cm^{-1} and Fe–O–Fe angle of 105.64(4)° were described, respectively. The correlations between the Fe–O–Fe angle and the J values are listed in Table 3 for di-μ-phenoxo-bridged dinuclear iron(III) complexes. From this, we can say that a crossover from ferromagnetism (S = 5) to antiferromagnetism (S = 0) has been observed at a Fe–O–Fe angle of ∼98°, like in the case for di-μ-hydroxo-bridged copper(II) complexes.[29]

Conclusions

The phenolic-oxygen-containing ligands, *N*-salicylidene-2-hydroxy-5-bromobenzylamine (H_2L^a), *N*-salicylidene-2-hydroxy-5-chlorobenzylamine (H_2L^b) or *N*-salicylidene-2-hydroxybenzylamine (H_2L^c), have proved to be good ligands for the synthesis of a series of di-μ-phenoxo-bridged dinuclear iron(III) complexes containing either two bridging groups (carboxylato, phosphato) or a chelating acetylacetonato group which cover the small Fe–O–Fe angle region in dinuclear iron(III) systems.

References

1 K. S. Murray, *Coord. Chem. Rev.*, **12**, 1 (1974).

2 a) S. J. Lippard, *Angew. Chem., Int. Ed. Engl.*, **27**, 344 (1988). b) I. M. Klotz and D. M. Kurtz, *Acc. Chem. Res.*, **17**, 16 (1984). c) P. C. Wilkins and R. G. Wilkins, *Coord. Chem. Rev.*, **79**, 195 (1987). d) J. B. Vincent, G. L. Oliver-Lilley, and B. A. Averill, *Chem. Rev.*, **90**, 1447 (1990). e) D. M. Kurtz, *Chem. Rev.*, **90**, 585 (1990).

3 "Magneto-Structural Correlations in Exchange Coupled Systems," ed by R. D. Willett, D. Gatteschi, and O. Kahn, Reidal Publishing Co., Dordrecht (1985).

4 a) S. M. Gorun and S. J. Lippard, *Inorg. Chem.*, **30**, 1625 (1991). b) J. R. Hart, A. K. Rappe, S. M. Gorun, and T. H. Upton, *Inorg. Chem.*, **31**, 5254 (1992). c) H. Weihe and H. U. Gudd, *J. Am. Chem. Soc.*, **119**, 6539 (1997).

5 a) M. G. B. Drew, V. McKee, and S. M. Nelson, *J. Chem. Soc., Dalton Trans.*, **1978**, 80. b) J. E. Plowman, T. M. Loehr, C. A. Schauer, and O. P. Anderson, *Inorg. Chem.*, **23**, 3553 (1984). c) R. N. Mukherjee, T. D. P. Stack, and R. H. Holm, *J. Am. Chem. Soc.*, **110**, 1850 (1988). d) P. Gomez-Romero, E. H. Witten, W. M. Reiff, G. Backes, J. Sanders-Loehr, and G. B. Jameson, *J. Am. Chem. Soc.*, **111**, 9039 (1989). e) P. Gomez-Romero, E. H. Witten, W. M. Reiff, and G. B. Jameson, *Inorg. Chem.*, **29**, 5211 (1990). f) G. Haselhorst, K. Wieghardt, S. Keller, and B. Schrader, *Inorg. Chem.*, **32**, 520 (1993). g) R. M. Buchanan, R. J. O'Brien, J. F. Richardson, and J.-M. Latour, *Inorg. Chim. Acta*,

214, 33 (1993). h) J. C. Plakatouras, T. Bakas, C. J. Huffman, J. C. Huffman, V. Papaefthymiou, and S. P. Perlepes, *J. Chem. Soc., Dalton Trans.*, **1994**, 2737. i) A. Hazell, K. B. Jensen, C. J. McKenzie, and H. Toftlund, *Inorg. Chem.*, **33**, 3127 (1994). j) M. Lausmann, I. Zimmer, J. Lex, H. Lueken, K. Wieghardt, and E. Vogel, *Angew. Chem., Int. Ed. Engl.*, **33**, 736 (1994). k) J. Li, J. Zou, M. Wu, Z. Xu, X. You, and T. W. Mak, *Polyhedron*, **14**, 23 (1995). l) J. Wang, M. S. Mashuta, Z. Sun, J. F. Richardson, D. N. Hendrickson, and R. M. Buchanan, *Inorg. Chem.*, **35**, 6642 (1996). m) G. Roelfes, M. Lubben, K. Chen, R. Y. N. Ho, A. Meetsma, S. Genseberger, R. M. Hermart, R. Hage, S. K. Mandal, V. G. Young, Y. Zang, H. Kooijman, A. L. Spek, L. Que, and B. L. Feringa, *Inorg. Chem.*, **38**, 1929 (1999). n) A.-R. Li, H.-H. Wei, and L.-L. Gang, *Inorg. Chim. Acta*, **290**, 51 (1999). o) Y.-G. Wei, S.-W. Zhang, and M.-C. Shao, *Polyhedron*, **16**, 2307 (1997). p) D. F. Xiang, X. S. Tan, S. W. Zhang, Y. Han, K. B. Yu, and W. X. Tang, *Polyhedron*, **17**, 2095 (1995). q) H. Matsushima, K. Iwasawa, K. Ide, M. Y. Reza, M. Koikawa, and T. Tokii, *Inorg. Chim. Acta*, **274**, 224 (1998).

6 H. Zheng, Y. Zang, Y. Dong, V. G. Young, and L. Que, *J. Am. Chem. Soc.*, **121**, 2226 (1999).

7 a) S. Yan, L. Que, L. F. Taylor, and O. P. Anderson, *J. Am. Chem. Soc.*, **110**, 5222 (1988). b) R. E. Norman, R. C. Holz, S. Menage, C. J. O'Connor, J. H. Zhang, and L. Que, *Inorg. Chem.*, **29**, 4629 (1990). c) R. E. Norman, S. Yan, L. Que, G. Backes, J. Ling, J. Sanders-Loehr, J. H. Zhang, and C. J. O'Conner, *J. Am. Chem. Soc.*, **112**, 1554 (1990). d) A. Hazell, K. B. Jensen, C. J. McKenzie, and H. Toftlund, *J. Chem. Soc., Dalton Trans.*, **1993**, 3249. e) N. Arulsamy, D. J. Hodgson, and J. Glerup, *Inorg. Chim. Acta*, **209**, 61 (1993). f) N. Arulsamy, P. A. Goodson, D. J. Hodgson, J. Glerup, and K. Michelsen, *Inorg. Chim. Acta*, **216**, 21 (1994). g) S. Wang, Q. Luo, X. Wang, L. Wang, and K. Yu, *J. Chem. Soc., Dalton Trans.*, **1995**, 2045. h) S. Yan, X. Pan, L. F. Taylor, J. H. Zhang, C. J. O'Connor, D. Britton, O. P. Anderson, and L. Que, *Inorg. Chim. Acta*, **243**, 1 (1996). i) B. Graham, B. Moubaraki, K. S. Murray, L. Spiccia, J. D. Cashion, and D. C. R. Hockless, *J. Chem. Soc., Dalton Trans.*, **1997**, 887. j) J. Glerup, K. Michelsen, N. Arulsamy, and D. J. Hodgson, *Inorg. Chim. Acta*, **274**, 155 (1998).

8 a) W. H. Armstrong, A. Spool, G. C. Papaefthymiou, R. B. Frankel, and S. J. Lippard, *J. Am. Chem. Soc.*, **106**, 3653 (1984). b) J. R. Hartman, R. L. Rardin, P. Chaudhuri, K. Pohl, K. Wieghardt, B. Nuber, J. Weiss, G. C. Papaefthymiou, R. B. Frankel, and S. J. Lippard, *J. Am. Chem. Soc.*, **109**, 7387 (1987). c) P. Gomez-Romero, N. Casan-Pastor, A. Ben-Hussein, and G. B. Jameson, *J. Am. Chem. Soc.*, **110**, 1988 (1988). d) J. B. Vincent, J. C. Huffman, G. Christou, Q. Li, M. A. Nanny, D. N. Hendrickson, R. H. Fong, and R. H. Fish, *J. Am. Chem. Soc.*, **110**, 6898 (1988). e) R. H. Beer, W. B. Tolman, S. G. Bott, and S. J. Lippard, *Inorg. Chem.*, **28**, 4557 (1989). f) X. Feng, S. G. Bott, and S. J. Lippard, *J. Am. Chem. Soc.*, **111**, 8046 (1989). g) R. H. Beer, W. B. Tolman, S. G. Bott, and S. J. Lippard, *Inorg. Chem.*, **30**, 2082 (1991). h) K. J. Oberhausen, J. F. Richardson, R. J. O'Brien, R. M. Buchanan, J. K. McCusker, R. J. Webb, and D. N. Hendrickson, *Inorg. Chem.*, **31**, 1125 (1992). i) M. Kotera, H. Shimakoshi, M. Nishimura, H. Okawa, S. Iijima, and K. Kano, *Inorg. Chem.*, **35**, 4967 (1996). j) V. A. Grillo, G. R. Hanson, T. W. Hambley, L. R. Gahan, K. S. Murray, and B. Moubaraki, *J. Chem. Soc., Dalton Trans.*, **1997**, 305.

9 T. Fujita, S. Ohba, Y. Nishida, and A. Goto, *Acta Crystallogr., Sect C*, **50**, 544 (1994).

10 S. Drueke, K. Wieghardt, B. Nuber, and J. Weiss, *Inorg. Chem.*, **28**, 1414 (1989).

11 R. C. Holz, T. E. Elgren, L. L. Pearce, J. H. Zhang, C. J. O'Connor, and L. Que, *Inorg. Chem.*, **32**, 5844 (1993).

12 S. Drueke, K. Wieghardt, B. Naber, J. Weiss, H.-P. Fleischhauer, S. Gehring, and W. Haase, *J. Am. Chem. Soc.*, **111**, 8622 (1989).

13 P. N. Turowski, W. H. Armstrong, M. E. Roth, and S. J. Lippard, *J. Am. Chem. Soc.*, **112**, 681 (1990).

14 a) J. A. Thich, C. C. Ou, D. Powers, B. Vasiliou, D. Mastropaolo, J. A. Potenza, and H. J. Schugar, *J. Am. Chem. Soc.*, **98**, 1425 (1976). b) C. C. Ou, R. A. Lalancette, J. A. Potenza, and H. J. Schugar, *J. Am. Chem. Soc.*, **100**, 2053 (1978). c) L. Borer, L. Thalken, C. Ceccarelli, M. Glick, J. H. Zhang, and W. M. Reiff, *Inorg. Chem.*, **22**, 1719 (1983). d) K. K. Nanda, S. K. Dutta, S. Baitalik, K. Venkatsubramanian, and K. Nag, *J. Chem. Soc., Dalton Trans.*, **1995**, 1239.

15 a) B. Chiari, O. Piovesana, T. Tarantelli, and P. F. Zanazzi, *Inorg. Chem.*, **21**, 1396 (1982). b) B. Chiari, O. Piovesana, T. Tarantelli, and P. F. Zanazzi, *Inorg. Chem.*, **23**, 3398 (1984). c) S. Menage and L. Que., Jr, *Inorg. Chem.*, **29**, 4293 (1990). d) G. D. Fallon, A. Markiewicz, K. S. Murray, and T. Quach, *J. Chem. Soc., Chem. Commun.*, **1991**, 198. e) M. Leluk, B. J. Trzebiatowska, T. Lis, *Polyhedron*, **11**, 1923 (1992). f) A. J. Blake, C. M. Grant, S. Parsons, G. A. Solan, and R. E. P. Winpenny, *J. Chem. Soc., Dalton Trans.*, **1996**, 321. g) F. L. Gall, F. F. Biani, A. Caneschi, P. Cinelli, A. Corma, A. C. Fabretti, and D. Gatteschi, *Inorg. Chim. Acta*, **262**, 123 (1997).

16 a) B. S. Snyder, G. S. Patterson, A. J. Abrahamson, and R. H. Holm, *J. Am. Chem. Soc.*, **111**, 5214 (1989). b) A. Elmali, Y. Elerman, I. Svoboda, and H. Fuess, *Acta Crystallogr.*, **C49**, 965 (1993).

17 a) P. N. Turowski, W. H. Armstrong, S. Liu, S. N. Brown, and S. J. Lippard, *Inorg. Chem.*, **33**, 636 (1994). b) B. Bremer, K. Schepers, P. Fleischhauer, W. Haase, G. Henkel, and B. Krebs, *J. Chem. Soc., Chem. Commun.*, **1991**, 510.

18 P. Chaudhuri, M. Winter, K. Wieghardt, S. Gehring, W. Haase, B. Nuber, and J. Weiss, *Inorg. Chem.*, **27**, 1564 (1988).

19 a) M. Mikuriya, S. Shigematsu, K. Kawano, T. Tokii, and H. Oshio, *Chem. Lett.*, **1990**, 729. b) M. Mikuriya, D. Jie, Y. Kakuta, and T. Tokii, *Bull. Chem. Soc. Jpn.*, **66**, 1132 (1993).

20 a) J. Dai, S. Akiyama, M. Munakata, and M. Mikuriya, *Polyhedron.*, **13**, 2495 (1994). b) J. Dai, H. Wang, and M. Mikuriya, *Polyhedron.*, **15**, 1801 (1996).

21 M. Mikuriya, Y. Kakuta, K. Kawano, and T. Tokii, *Chem. Lett.*, **1991**, 2031.

22 L. C. Raiford and E. P. Clark, *J. Am. Chem. Soc.*, **45**, 1738 (1923).

23 M. Yamaguchi, *Nippon Kagaku Zasshi*, **73**, 393 (1952).

24 P. W. Selwood, "Magnetochemistry," Interscience Publishers, New York (1956), pp. 78, 91.

25 B. A. Frenz, "The SDP-User's Guide,"Enraf-Nonius, Delft, The Netherlands (1985).

26 K. Nakamoto, "Infrared and Raman Spectra of Inorganic and Coordination Compounds," 4th ed, Wiley interscience, New York (1986).

27 a) N. Torihara, M. Mikuriya, H. Okawa, and S. Kida, *Bull. Chem. Soc. Jpn.*, **53**, 1610 (1980). b) M. Mikuriya, N. Torihara, H. Okawa, and S. Kida, *Bull. Chem. Soc. Jpn.*, **54**, 1063 (1981).

28 H. J. Schugar, G. R. Rossman, J. Thibeault, and H. B. Gray, *Chem. Phys. Lett.*, **6**, 26 (1970).

29 a) D. J. Hodgson, *Prog. Inorg. Chem.*, **19**, 173 (1975). b) W. E. Hatfield, "Theory and Applications of Molecular Paramagnetism," ed by E. A. Boudreaux and L. N. Mulay, Wiley-Interscience, New York (1976).